Electronic Supplementary Material (ESI) for Chemical Communications.

Supporting Information for

An Upper Bound Visualization of Design Trade-Offs in Adsorbent Materials for Gas Separations: Alkene/Alkane Adsorbents

Ahmed H. Elashkar,[a,†] Gavin Hedley,[a,†] Omid T. Qazvini,[b] Shane G. Telfer,[c] and Matthew G. Cowan [a,]*

Supporting Information

Contents

Table of terms

Terms/Symbols	Definition	Units
Gas *i*	A gas with relatively high affinity for an adsorbent material	
Gas *j*	A gas with relatively low affinity for an adsorbent material	
Capacity	The amount of gas adsorbed at equilibrium	$mmol_i \cdot g^{-1}$ equivalent to: $mol \cdot kg^{-1}$
Selectivity (α_{ij})	$\frac{\text{Amount of gas } i \text{ adsorbed}}{\text{Amount of gas } j \text{ adsorbed}}$	$\frac{mol_i}{mol_j}$
Heat of adsorption (ΔH)	Amount of energy released by the adsorption of a gas molecule. Equivalent to the amount of energy required to desorb a gas molecule.	$kJ \cdot mol^{-1}$
Θ_i	Proportion of available sites occupied by gas *i*	$\frac{mol_{occupied}}{mol_{unoccupied}}$
K_{eq}^{i}	Equilibrium constant for the adsorption of gas *i*. $\frac{[\text{Occupied sites}]}{[\text{Gas}][\text{Unoccupied sites}]}$	
p_i	partial pressure of gas *i*	kPa
n_i	total amount of gas *i* adsorbed on the adsorbent surface	
m^1	The saturation capacity on site '1' of a heterogeneous adsorbent	
m^2	The saturation capacity on site '2' of a heterogeneous adsorbent	
b_i	Affinity parameters for gas *i* on adsorption site b of a heterogeneous adsorbent	
d_i	Affinity parameters for gas *i* on adsorption site d of a heterogeneous adsorbent	
y_i	mol fractions of gas *i* in the gas phase	$\frac{mol_i}{mol_{total}}$
y_j	mol fractions of gas *j* in the gas phase	$\frac{mol_j}{mol_{total}}$
T	Temperature	K
$Q_i^{(b)}$	Heat of adsorption of gas *i* on site b of a heterogeneous adsorbent	$kJ \cdot mol^{-1}$
$Q_i^{(d)}$	Heat of adsorption of gas *i* on site d of a heterogeneous adsorbent	$kJ \cdot mol^{-1}$

1. Search method

We performed the search for this review using the 'research topic' function of the SciFinder database.

Keywords included: "Adsorption of olefins"; "Adsorption of alkenes"; "Olefins adsorption on porous adsorbents"; "Alkenes adsorption on porous adsorbents"; "Adsorption of ethylene/ethane"; "Adsorption of ethene/ethane"; "Adsorption of propylene/propane"; "Adsorption of propene/propane"; "Adsorption of butylene/butane"; "Adsorption of butene/butane"; "Adsorption of olefins on copper"; "Adsorption of alkenes on copper"; "Adsorption of olefins by small molecule adsorbents"; "Adsorption of alkenes by small molecule adsorbents"; "Olefins adsorption on nonporous adsorbents"; "Alkenes adsorption on nonporous adsorbents"; "Adsorption of ethylene/ethane on copper"; "Adsorption of ethene/ethane on copper"; "Adsorption of propylene/propane on copper"; "Adsorption of propene/propane on copper"; "Adsorption of butylene/butane on copper"; "Adsorption of butene/butane on copper"; "Adsorption of ethylene/ethane on silver"; "Adsorption of ethene/ethane on silver"; "Adsorption of propylene/propane on silver"; "Adsorption of propene/propane on silver"; "Adsorption of butylene/butane on silver" and "Adsorption of butene/butane on silver".

Results of these keywords were combined, refined by 'language' to 'English', by 'document type' to 'journal' and 'book' and by 'year' to '2000-2020'. Finally, Duplicates were removed, and the final number of references were checked. The results were judged based on their titles and abstracts and all relevant papers were examined in detail and included in this review.

2. Summary of literature searches

2.1 Ethene selective adsorbents

Table S1. Comparison between the ethene uptake, ethene/ethane selectivity, and heat of adsorption of the ethene selective porous adsorbents reported in this review.

Material	Ethene Uptake ($mmol_{ethene}/g_{material}$)	Temperature (K)	Pressure (kPa)	Ethene/ethane Selectivity	Heat of Adsorption (kJ/mol)	Reference
Diamondyne	14.5	298	1000	1.8[d] – 2.7[a]	-32.67[e]	1
Kureha carbon	10.2	194	120	1.07[d] – 1.6[a]	-29.5[b]	2
13X zeolite binderless	4.25	323	500	1.2[d] – 2[a]	–	3
13X zeolite binderless	3.7	323	100	1.45[d] – 2.2[a]	-30[b]	3
UTSA-33a	3.62	296	101	1.35[d]	-31[b]	4
13X zeolite	3.32	298	101	12[a]	-41.5[f]	5
13X-APG	3.23[g]	298	100	1.29[d]	-35.2[g]	6
Zeolite 13X pellet	2.9	298	600	1.12[d]	–	7
Zeolite 13X pellet	2.68	298	100	1.43[d]	–	7
HY zeolite	2.65	303	500	4.5[a]	–	8
UTSA-280	2.5	298	101	>10000[a]	-34.1[b]	9
Zeolite 5A	2.45	303	101	4.5[a]	-37[c]	10
MIL-101	2.22	303	101	1.21[d] – 2[a]	-25.5[b]	11
MIL-101	2.15	298	100	1.1[a]	-9[b]	12
$[Zn_2(fm)_2(bpy)]_n$	1.9	298	600	3.4[d]	–	7
HY zeolite	1.75	303	100	4.5[a]	–	8
MPI	1.6	298	101	0.9[a]	-32.5[b]	13
KIT-6	1.53	303	700	1.21[d]	–	14
NUS-36	1.5	298	101	4.1[a]	-44[b]	15
SBA-15	1.49	303	700	1.18[d]	–	14
$A_{10}B_1$	1.42	298	80	1.5[a]	–	16
Silica	1.2	299	101	1.46[d]	-25.5[k]	17
HMS type mesoporous silica	0.89	303	101	1.6[d]	35.1[b]	18
Silica SBA-15	0.89	303	101	1.6[d]	8.4[b]	19
Ca-ETS-4	0.86	303	600	1.22[d]	–	20
SYSG	0.76	303	700	1.1[d]	–	14
MPI-S	0.75	298	101	1.4[a]	-35[b]	13
Ca-ETS-4	0.6	303	100	1.58[d]	–	20
HOF-4	0.5	296	100	14[a]	-44[b]	21
SBA-15	0.45	303	100	1.4[d]	–	14
$[Zn_2(fm)_2(bpy)]_n$	0.4	298	100	1.8[d]	–	7
MCM-48	0.38	303	100	2.2[d]	–	22
KIT-6	0.36	303	100	1.36[d]	–	14
SiO_2	0.36	343	101	1.5[d]	–	23
SYSG	0.18	303	100	1.18[d]	–	14

[a] Calculated using ideally absorbed solution theory (IAST) for an equimolar amount of ethene and ethane at the responding temperature and pressure. [b] Calculated by applying Clausius−Clapeyron equation to adsorption isotherms at different temperatures (value shown is at low surface coverage). [c] Highest Q_{st} value at different surface coverage. [d] Determined from reported adsorption capacities of both gases (ethene/ethane uptake ratio). [e] Measurement method not

shown/available. [f] Calculated by using the virial equation. [g] Measured/calculated using unconventional method, check the reference for details.

Table S2. Comparison between the ethene uptake, ethene/ethane selectivity, and heat of adsorption of the ethene selective porous with open metal sites adsorbents reported in this review.

Material	Ethene Uptake ($mmol_{ethene}/g_{material}$)	Temperature (K)	Pressure (kPa)	Ethene/ethane Selectivity	Heat of Adsorption (kJ/mol)	Reference
Cu-BTC bead	7.5	323	700	1.09[d] – 1.2[a]	-26.69[b]	24
Powder Mg-MOF-74	7.37	298	101	5.5[a]	-38.6[f]	5
Mg-MOF-74	7.2	298	100	15.3	-42.5[b]	25
Co_2(m-dobdc)	7	298	101	15[a]	-47.5[b]	26
Fe_2(m-dobdc)	7	298	101	25[a]	-56[b]	26
Co-MOF-74	6.9	298	101	1.1[d] – 8.2[a]	–	27
Mg_2(dhtp)	6.9	295	101	1.2[d]	–	28
Mn_2(m-dobdc)	6.7	298	101	17[a]	-49.5[b]	26
Ni_2(m-dobdc)	6.6	298	101	15.5[a]	-55[b]	26
MgMOF-74	6.4	296	101	5.63[a]	-45.2[b]	29
Mn_2(dobdc)	6.33	318	101	8.13[a]	-44[b]	30
CoMOF-74	6.3	296	101	6.45[a]	-41[b]	29
Fe_2(dobdc)	6.3	318	101	13.6[a]	-46[b]	30
Mg_2(dobdc)	6.24	318	101	4.44[a]	-42[b]	30
Co_2(dobdc)	6.07	318	101	5.82[a]	-44[b]	30
Molded Mg-MOF-74	6.06	298	101	6[a]	-42[f]	5
Fe_2(dobdc)	6.02	318	101	18[a]	-45[b]	31
Ni_2(dobdc)	6.01	318	101	5.93[a]	–	30
Zn_2(dobdc)	5.38	318	101	2.7[a]	-36[b]	30
Co_2(dhtp)	4.6	295	101	1.15[d]	–	28
Cu-BTC bead	4.5	323	100	1.29[d] – 1.5[a]	-26.69[b]	24
PAF-1-SO3Ag	4	296	101	27[a]	–	32
MIL-100(Fe)	3.8	298	101	10[a]	-83[b]	33
$Zn_2Cu_3(BTDD)_3$	3.76	296	101	1.36[d]	-79.9[e]	34
$Zn_{2.7}Cu_{2.3}(BTDD)_3$	3.58	296	101	1.36[d]	-81[e]	34
Cr_^{t}Bu-bdc	3.51	298	101	1.15[d]	-33[b]	35
$Zn_{2.8}Cu_{2.2}(BTDD)_3$	3.41	296	101	1.21[d]	-79.5[e]	34
MC-S-Ag-3	3.4	298	101	2.5[a]	–	36
1.6AgM-DS	3.37	298	100	9.5[a]	-59.2[b]	12
4CuCl/CMK-3	3.18	303	100	1.84[d]	-53[b]	37
MIL-101–Cr–SO_3Ag	2.81	318	100	9.7[a]	-63[b]	38
MIL-101(Cr)_DAA	2.8	303	101	1.6[a]	–	39
(Cr)-MIL-101-SO_3Ag	2.61	303	101	16[a]	-120[b]	40
Cu(OPTz), **1a**	2.6	298	101	4.5[d]	-27.7[b]	41
1.6AgM-WI	2.5	298	100	8.1[a]	–	12
Silver faujasite zeolite (AgX)	2.46	303	100	2.5[d]	–	42
MIL-101(Cr)	2.4	303	101	1.25[a]	–	39
PAF-40-Fe	2.31	298	110	1.25[d]	-30[f]	43
Na-ETS-10	2.25	298	800	1.18[d] – 15.9[a]	-49.7[b]	44
Li-ETS-10	2.2	298	100	1.26[d] – 6[a]	–	45
PAF-40-Mn	2.18	298	110	1.06[d]	-25.1[f]	43
Na-ETS-10	2.1	303	101	1.24[d] – 5[g]	-49.6[b]	46

NUS-6(Hf)-Ag	2.02	298	105.8	6[a]	-56.5[f]	[47]
Ba/H-ETS-10	2	298	100	1.25[d] – 2.5[a]	–	[45]
Ba-ETS-10	1.9	298	100	1.19[d] – 3.35[a]	–	[45]
CPL-1	1.83	273	600	7.5[d]	–	[48]
Cu^{I}@UiO-66-$(COOH)_2$	1.8	298	101	80.8[a]	-48.5[b]	[49]
La/H-ETS-10	1.8	298	100	1.16[d] – 1.8[a]	–	[45]
$CuA_{10}B_1$	1.77	298	80	3.8[a]	–	[16]
(Cr)-MIL-101-SO_3H	1.7	303	101	1.2[a]	-35[b]	[40]
Na-ETS-10	1.7	298	100	1.2[d] – 17[a]	–	[45]
Ag/KIT-6	1.68	303	700	1.76[d]	–	[47]
Ag/SBA-15	1.67	303	700	2[d]	–	[47]
MIL-101–Cr–SO3H	1.65	318	100	1.2[a]	-10[b]	[38]
Zn-ETS-4	1.5	298	100	1.5[d] – 5[a]	–	[50]
50Cu	1.47	348	650	4.13[d]	–	[51]
2Ce50Cu	1.45	348	650	3.61[d]	–	[51]
K-ETS-10	1.4	298	100	1.27[d] – 9.7[a]	–	[45]
Zn-RPZ	1.31	298	100	1.64[d] – 14[a]	–	[50]
Olesorb-1	1.17	303	101	8.6[d]	56.48[b]	[52]
Ag^+ Resin	1.15	298	101	9.2[d]	-41.84[c]	[53]
5Ce50Cu	1.12	348	650	8.3[d]	–	[51]
8Ce50Cu	1.12	348	650	6.25[d]	–	[51]
10Ce50Cu	1.12	348	650	5.89[d]	–	[51]
Ag-ETS-10	1.1	298	100	1.1[d]	–	[45]
Ag/SYSG	1.1	303	700	1.9[d]	–	[47]
Ag–SBA-15	1.08	303	100	21.3[a]	-22.5[b]	[54]
Cu-ETS-10	1	298	100	1.4[d] – 3.85[a]	–	[45]
Ag^+-exchanged S9	0.992	298	101	3.56[d]	–	[55]
Ag–TUD-1	0.91	303	100	14.2[a]	-22.8[b]	[54]
10 wt.% Ag/CPL-2	0.9	298	101	26.1[a]	-42.9[b]	[56]
Ba-ETS	0.9	298	100	3[d] – 63[a]	–	[50]
Ca/H-ETS	0.9	298	100	2.4[d] – 40[a]	–	[50]
Ca/H-R	0.9	298	100	2.14[d] – 9.5[a]	–	[50]
1.6AgM-SG	0.87	298	100	1.8[a]	–	[12]
Ag–KIT-6	0.85	303	100	16.4[a]	-24.2[b]	[54]
50Cu	0.84	348	100	9.5[d]	–	[51]
MPI-Ag	0.82	298	101	3.1[a]	-37.1[b]	[13]
Ag/SBA-15	0.76	303	100	5.83[d]	–	[47]
Ag/KIT-6	0.72	303	100	4[d]	–	[47]
2Ce50Cu	0.69	348	100	5.17[d]	–	[51]
5Ce50Cu	0.625	348	100	14[d]	–	[51]
Sr-ETS	0.62	298	100	2.48[d] – 52[a]	–	[50]
Sr-RPZ	0.6	298	100	2[d] – 17[a]	–	[50]
Ag–Amberlyst 35	0.56	303	100	60.8[a]	-21.8[b]	[54]
Ag/SYSG	0.54	303	100	5.89[d]	–	[47]
8Ce50Cu	0.49	348	100	11[d]	–	[51]
10Ce50Cu	0.49	348	100	11[d]	–	[51]
10Cu-MCM-48	0.49	303	100	3.6[d]	–	[22]
5Cu-MCM-48	0.45	303	100	3.3[d]	–	[22]
Ba-RPZ	0.4	298	100	1.38[d] – 9.5[a]	–	[50]
20Cu-MCM-48	0.3	303	100	2[d]	–	[22]

[a] Calculated using ideally absorbed solution theory (IAST) for an equimolar amount of ethene and ethane at the responding temperature and pressure. [b] Calculated by applying Clausius−Clapeyron equation to adsorption isotherms at different temperatures (value shown is at low surface coverage). [c] Measurement method not shown/available. [d] Determined from reported adsorption capacities of both gases (ethene/ethane uptake ratio). [e] Determined from

temperature-programmed desorption (TPD) measurements. [f] Calculated by using the virial equation. [g] Determined from breakthrough data. [h] Measured/calculated using unconventional method, check the reference for details.

Table S3. Comparison between the ethene uptake, ethene/ethane selectivity, and heat of adsorption of the ethene selective nonporous adsorbents reported in this review.

Material	Ethene Uptake ($mmol_{ethene}/g_{material}$)	Temperature (K)	Pressure (kPa)	Ethene/ethane Selectivity	Heat of Adsorption (kJ/mol)	Reference
Ag^{I}-coordinated phenanthro-line-based polymer (**4**)	5.04	298	101	14.8[f]	–	57
CuCl(8.0)/AC	3.6	303	500	59[f]	–	58
8CuCl/CMK-3	3.55	303	100	2.67[a]	-67[b]	37
4CuCl/CMK-3	3.18	303	100	1.84[a]	-53[b]	37
[Cu-H]$_3$	3.13[c]	293	636	47[d]	-15.3[b]	59
[(3,4,5-$(CF_3)_3$Pz)Cu]$_3$	2.76	293	100	136[a]	-13.1[b]	60
36 wt% CuCl/NaX	2.7	373	300	2.7[a]	–	61
CuCl(8.0)/AC	2.57	303	100	69.42[f]	-60.8[b]	58
40 wt% Cu^{+}@MIL-101	2.46	303	101	2.02[a] – 6.2[f]	-40[b]	11
[Cu-Br]$_3$	2.42	293	100	46.5[a]	-9.6[b]	59
[Ag^{I}(2,2'-bipyridine)][BF_4]	2.38	293	90	390[a]	-54[g]	62
CuCl(5.0)@HY	2.3	303	500	58[f]	–	8
[Ag^{I}(6,6'-dimethyl-2,2'-bipyridine)][OTf]	2.18	293	90	340[a]	-55[g]	62
CuCl(5.0)@HY	2.14	303	100	67[f]	-70.2[b]	8
36 wt% CuCl/NaX	1.9	373	100	4.2[a]	–	61
$AgNO_3$/clay adsorbent	1.15	298	101	8.2[a]	–	63
$AgNO_3$/clay	1.1[e]	353	120	22[a]	36.9[h]	64
$AgNO_3/SiO_2$ (impregnation)	0.91	343	101	4.5[a]	–	23
36.7% $CuCl_2$/CSC	0.84[e]	313	100	7.6[e]	–	65
CuCl/γ-Al_2O_3	0.73	298	101	7.3[e]	-48.95[h]	53
$AgNO_3/SiO_2$ (dispersion)	0.5	343	101	4[a]	–	23
1 (fine crystal)	0.15	298	100	190[a]	-32[b]	66

[a] Determined from reported adsorption capacities of both gases (ethene/ethane uptake ratio). [b] Calculated by applying Clausius−Clapeyron equation to adsorption isotherms at different temperatures. [c] Pressure drop method for 120 min. [d] Selectivity calculated from capacities measured by pressure drop method. [e] Determined from breakthrough data. [f] Calculated using ideally absorbed solution theory (IAST) for an equimolar amount of ethene and ethane at the responding temperature and pressure. [g] Measured using differential scanning calorimetry (DSC). [h] Measurement method not shown/available.

2.2 Ethane selective adsorbents

Table S4. Comparison between the ethane uptake, ethane/ethene selectivity, and heat of adsorption of the ethane selective porous adsorbents reported in this review.

Material	Ethane Uptake ($mmol_{ethane}/g_{material}$)	Temperature (K)	Pressure (kPa)	Ethane/ethene Selectivity	Heat of Adsorption (kJ/mol)	Reference
3D Ni(BT)-M	4.2	298	101	1.2[c]	-23.6[b]	67
3D ZIF-7-M	2.8	298	101	1.9[c]	-40.8[b]	67
5Ce	1.12	348	100	1.14[a]	–	51
5Ce	2.72	348	650	1.05[a]	–	51
AlMePO-α	0.35[e]	298	101	4[e]	–	68
C-600-3	6.1	298	100	1.15[a] – 2[c]	–	69
C-700-3	7.2	298	100	1.22[a] – 2.5[c]	-33[b]	69
C-800-3	7.1	298	100	1.27[a] – 2.2[c]	–	69
C-800-4	6.6	298	100	1.29[a] – 1.9[c]	–	69
C-800-5	5	298	100	1.28[a] – 1.75[c]	–	69
CMK-3	3.11	303	100	1.08[a]	-20[b]	37
C-PDA-2	7.93	298	101	1.2[a] – 1.75[c]	–	70
C-PDA-3	6.57	298	101	1.29[a] – 1.9[c]	-22.2[b]	70
C-PDA-3	9.41	273	101	1.24[a]	–	70
C-PDA-4	5.68	298	101	1.28[a] – 1.53[c]	–	70
C-PDA-5	4.86	298	101	1.26[a] – 1.5[c]	–	70
HiSiv 3000	1.63[h]	298	100	1.02[a]	-33.5[g]	6
IFP-1	2.9	303	101	1.12[a]	-29.3[f]	71
IFP-3	1.5	303	101	1.11[a]	-28.3[f]	71
IFP-5	2.2	303	101	1.05[a]	-28.6[f]	71
IRMOF-8	4	298	101	1.75[c]	-52[b]	72
JNU-2	4.19	298	101	1.18[a]	-29.4[b]	73
Kureha carbon	8	194	10	1.11[a]	-28.2[b]	2
MAF-49	1.7	316	101	9[c]	-60[d]	74
MIL-53(Al)-FA	3.7	308	100	1.9[c]	–	75
MIL-101	14.6	298	800	1.2[a]	-30[b]	76
MIL-101a	8.8	298	800	1.13[a]	-23[b]	76
MIL-101b	9.25	298	800	1.09[a]	-27[b]	76
MUF-15	4.69	293	101	1.96[c]	–	77
$Ni(bdc)(ted)_{0.5}$	5	298	101	1.47[a]	-21.5[d]	78
Norit R1 Extra	4.33[h]	298	100	1.17[a]	-27.8[g]	6
PAF-40	1.95	298	110	1.08[a]	-36[d]	43
PAF-302	31.8	298	1000	1.14[a] – 1.7[c]	-33.87[i]	1
PCN-245	3.27	298	100	1.8[c]	-23[b]	79
TJT-100	3.84	298	101	1.2[c]	-29[b]	80
UiO-66-ADC	1.6	298	101	1.8[c]	-36[b]	15
ZIF-4	2.3	293	101	1.05[a] – 1.5[c]	–	81
ZIF-4	2.35	293	100	1.09[a] – 1.75[c]	–	82
ZIF-7	1.75	298	50	1.4[a]	–	83
ZIF-7	1.92	298	100	1.04[a] – 2.4[c]	-27[b]	84
ZIF-8	5.8	308	101	1.16[a]	-20[f]	85

ZIF-8	2.55	293	101	1.67[a]	–	[28]
ZIF-9	2.44	293	101	1.02[a]	-46.72[h]	[86]
ZIF-67	6	308	101	1.15[a]	-21[f]	[85]
ZIF-71	1.4	293	101	1.27[a]	-27.5[h]	[86]
$Zn_5Cl_4(BTDD)_3$	4	296	101	1.57[a]	–	[34]

[a] Determined from reported adsorption capacities of both gases (ethane/ethene uptake ratio). [b] Calculated by applying Clausius−Clapeyron equation to adsorption isotherms at different temperatures (value shown is at low surface coverage). [c] Calculated using ideally absorbed solution theory (IAST) for an equimolar amount of ethane and ethene at the responding temperature and pressure. [d] Calculated by using the virial equation. [e] Measured using OPLS-UA model. [f] Calculated from the Widom Insertion Method. [g] Measured/calculated using unconventional method, check the reference for details. [h] Obtained from simulations based on the UFF. [i] Measurement method not shown/available.

Table S5. Comparison between the ethane uptake, ethane/ethene selectivity, and heat of adsorption of the ethane selective porous with open metal sites adsorbents reported in this review.

Material	**Ethane Uptake ($mmol_{ethane}/g_{material}$)**	**Temperature (K)**	**Pressure (kPa)**	**Ethane/ethene Selectivity**	**Heat of Adsorption (kJ/mol)**	**Reference**
Cu–BTC	6	298	100	1.2[a] – 2.1[c]	–	[87]
Cu-MOF1	2.9	298	101	1.45[a]	-34.5[b]	[88]
$Zn_{3.8}Cu_{1.2}(BTDD)_3$	3.23	296	101	1.15[a]	–	[34]

[a] Determined from reported adsorption capacities of both gases (ethane/ethene uptake ratio). [b] Calculated by applying Clausius−Clapeyron equation to adsorption isotherms at different temperatures (value shown is at low surface coverage). [c] Calculated using ideally absorbed solution theory (IAST) for an equimolar amount of ethane and ethene at the responding temperature and pressure.

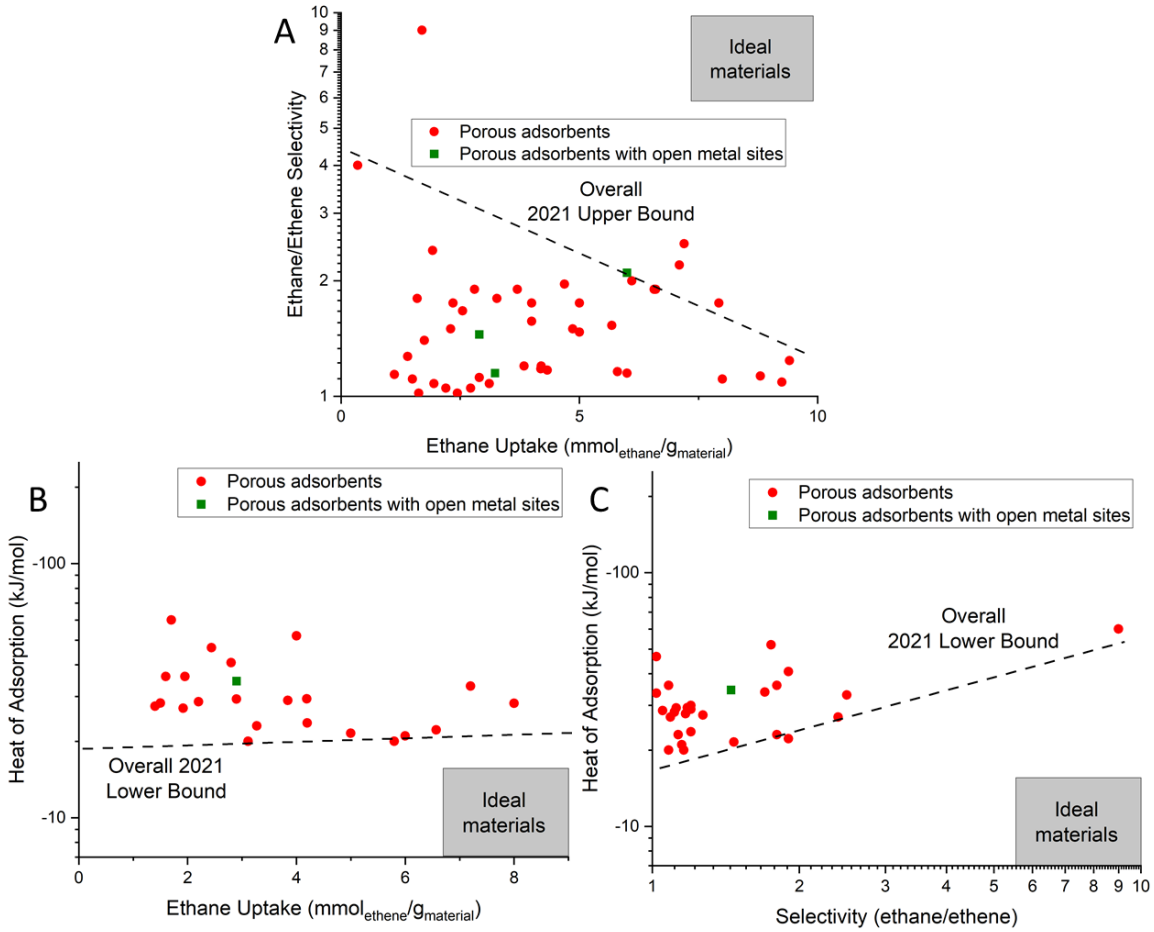

Figure S1. Bound plots for ethane selective adsorbents. A) Upper bound correlation illustrating the trade-off between uptake and selectivity in adsorbents characterized for ethane/ethene separations. Line equation: y = -0.319x + 4.40. B) Lower bound correlations illustrating the trade-off between uptake and heat of adsorption in adsorbents characterized for ethane/ethene separations. Line equation: y = 0.323x + 18.7. C) Lower bound correlation illustrating the trade-off between selectivity and heat of adsorption in adsorbents characterized for ethane/ethene separations. Line equation: y = 4.44x – 12.3.

2.3 Breakthrough data for adsorbents used for ethene/ethane separation

Table S6. Breakthrough data for ethene selective adsorbents reported in this review.

Material	Temperature (K)	Pressure (kPa)	Breakthrough Time (min) Ethane / Ethene	Alkene Productivity (L/Kg)	Ethene Heat of Adsorption (kJ/mol)	Reference
10 wt.% Ag/CPL-2	298	101	5 /6[a]	–	-42.9[k]	56
36 wt% CuCl/NaX	358	200	2.45 / 9.9[s]	–	–	61
40 wt% Cu^{+}@MIL-101	303	101	12 / 24.5[a]	–	-40[k]	11
13X zeolite binderless	373	150	9.2 / 22	–	-30[k]	3
$AgNO_3$/clay	353	120	3.08 / 7[t]	2.75[i,m]	-36.9[l]	64
Co_2(dhtp)	295	101	65 / 89[a]	–	–	28
Co_2(m-dobdc)	318	101	3 / 46[a]	–	-47.5[k]	26
CoMOF-74	296	100	60 / 100[c]	4.47[i,j]	-41[k]	29
CPL-1	273	800	40 / 60[a]	23[b]	–	48
Cu^{I}@UiO-66-$(COOH)_2$	298	100	33 / 86[d]	43[e]	-48.5[k]	49
Fe_2(dobdc)	318	100	18 / 32[a]	5[i,j]	-45[k]	31
FeMOF-74	318	100	–	4.98[i,j]	-47[k]	29
HOF-4	296	100	2 / 6[c]	–	-44[k]	21
MC-S-Ag-3	298	100	210 / 310[c]	–	–	36
Mg_2(dhtp)	295	101	17 / 21[a]	–	–	28
MgMOF-74	296	100	47 / 80[c]	3.72[i,j]	-45.2[k]	29
MIL-101	303	101	12.5 / 13.5[a]	–	-25.5[k]	11
MIL-101–Cr–SO3Ag	296	100	11 / 25[a]	–	-63[k]	38
Mn_2(m-dobdc)	298	101	13 / 37[a]	–	-49.5[k]	26
Na-ETS-10	298	101	4 / 6[q]	–	-49.6[k]	46
NUS-6(Hf)-Ag	298	101	5.83 / 11.67[a]	16.8[b]	-56.5[r]	47
NUS-36	298	101	11 / 19[a]	–	-44[k]	15
Olesorb-1	295	125	–	1.4[m,p]	-56.48[k]	52
Silver faujasite zeolite (AgX)	303	100	4 / 11[n]	–	–	42
Silver zeolite A (AgA)	303	100	0.05 / 15[n]	–	–	42
UTSA-280	298	101	12 / 105[a]	41.7[h]	-34.1[k]	9
Zeolite 13X pellet	298	800	26 / 47[a]	–	–	7
Zn_2Cu_3(BTDD)$_3$	296	101	0.2 / 3.2[a]	16.4[f]	-79.9[t]	34
$[Zn_2(fm)_2(bpy)]_n$	298	800	20 / 31[a]	–	–	7

[a] Breakthrough cycle of equimolar alkane/alkene (50:50) mixture. [b] Purity not shown/available. [c] Dimensionless time. [d] Specific breakthrough time (min/g). [e] Purity over 92.5%. [f] Purity over 99.99%. [g] Purity over 99.95%. [h] Purity over 99.2%.

[i] Purity over 99.5%. [j] Productivity is expressed as mol of alkene per L of adsorbent. [k] Calculated by applying Clausius−Clapeyron equation to adsorption isotherms at different temperatures (value shown is at low surface coverage). [l] Measurement method not shown/available. [m] Productivity is expressed as mol of alkene per kg of adsorbent per hour. [n] Breakthrough cycle of a mixture of ethane/ethene/nitrogen (10:10:80). [o] Calculated from the Widom Insertion Method. [p] Purity over 99.8%. [q] Breakthrough cycle of a mixture of 41% ethane and 59% ethene. [r] Calculated by using the virial equation. [s] Breakthrough cycle of a mixture of alkane/alkene/helium (25:25:50). [t] Determined from temperature-programmed desorption (TPD) measurements. [u] Purity of 97%. [v] Purity of 98%.

Table S7. Breakthrough data for ethane selective adsorbents reported in this review.

Material	Temperature (K)	Pressure (kPa)	Breakthrough Time (min) Ethane / Ethene	Alkene Productivity (L/Kg)	Ethane Heat of Adsorption (kJ/mol)	Reference
C-700-3	298	100	6.4 / 4[a]	–	-33[k]	[69]
C-800-3	298	100	7 / 4.5[a]	–	–	[69]
$Fe_2(O_2)$(dobdc)	298	101	55 / 22[a]	17.7[f]	-66.8[k]	[89]
IFP-1	303	101	17 / 12[a]	–	-29.3[o]	[71]
IFP-3	303	101	5 / 3[a]	–	-28.3[o]	[71]
IFP-5	303	101	10 / 7[a]	–	-28.6[o]	[71]
JNU-2	298	101	99 / 69[d]	21.2[f]	-29.4[k]	[73]
MAF-49	316	101	350 / 248[a]	6.27[g]	-60[r]	[74]
MUF-15	293	101	–	16[b]	–	[77]
PCN-245	298	100	7.5 / 6.3[a]	–	-23[k]	[79]
ZIF-4	293	101	33 / 13[a]	–	–	[81]
ZIF-7	298	200	21 / 4[a]	–	-27[k]	[84]
ZIF-8	295	101	20 / 18[a]	–	–	[28]

[a] Breakthrough cycle of equimolar alkane/alkene (50:50) mixture. [b] Purity not shown/available. [c] Dimensionless time. [d] Specific breakthrough time (min/g). [e] Purity over 92.5%. [f] Purity over 99.99%. [g] Purity over 99.95%. [h] Purity over 99.2%. [i] Purity over 99.5%. [j] Productivity is expressed as mol of alkene per L of adsorbent. [k] Calculated by applying Clausius−Clapeyron equation to adsorption isotherms at different temperatures (value shown is at low surface coverage). [l] Measurement method not shown/available. [m] Productivity is expressed as mol of alkene per kg of adsorbent per hour. [n] Breakthrough cycle of a mixture of ethane/ethene/nitrogen (10:10:80). [o] Calculated from the Widom Insertion Method. [p] Purity over 99.8%. [q] Breakthrough cycle of a mixture of 41% ethane and 59% ethene. [r] Calculated by using the virial equation. [s] Breakthrough cycle of a mixture of alkane/alkene/helium (25:25:50). [t] Determined from temperature-programmed desorption (TPD) measurements. [u] Purity of 97%. [v] Purity of 98%.

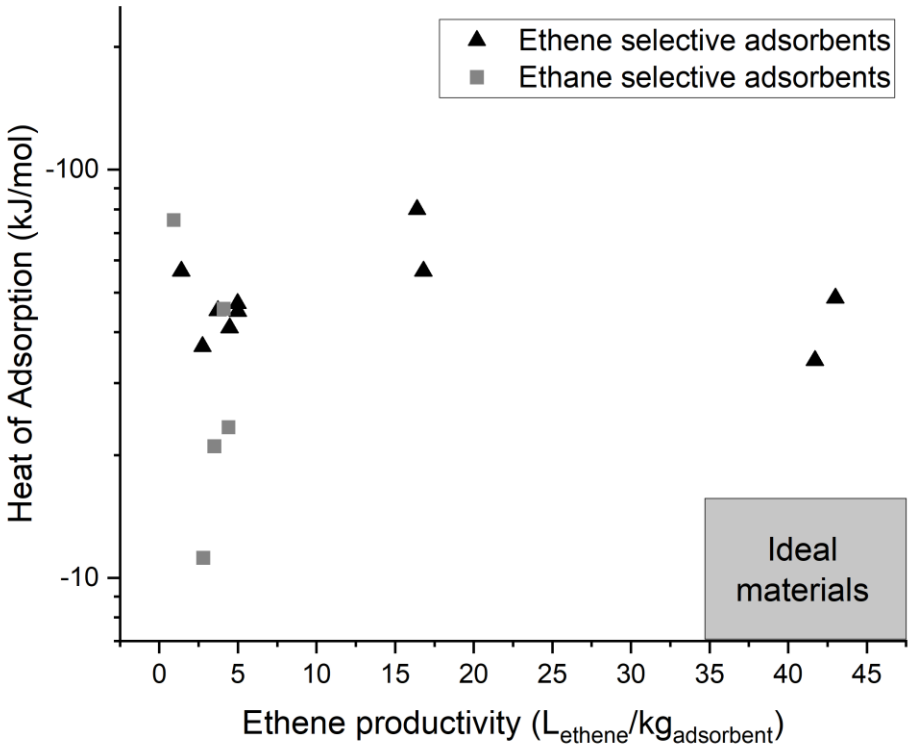

Figure S2. Bound plot for ethene and ethane selective adsorbents tested for breakthrough measurements. Note that no real conclusions can be drawn from this data due to the variance in measurement conditions and judgement of the purity that defines 'breakthrough.'

2.4 Propene selective adsorbents

Table S8. Comparison between the propene uptake, propene/propane selectivity, and heat of adsorption of the propene selective porous adsorbents reported in this review.

Material	Propene Uptake ($mmol_{propene}/g_{material}$)	Temperature (K)	Pressure (kPa)	Propene/Propane Selectivity	Heat of Adsorption ($kJ/mol_{propene}$)	Reference
PAF-302	32	298	1000	1.06[a] – 1.5[f]	-15.99[j]	[1]
Diamondyne	10.3	298	1000	1.16[a] – 2.65[f]	-10.91[j]	[1]
Kureha carbon	7	273	120	1.15[a] – 1.1[f]	-38.3[b]	[2]
Norit R1 Extra	5.73[c]	298	100	1.03[a]	-41.4[d]	[6]
ZIF-67	4.22	273	100	1.1[a]	–	[90]
ZIF-67	4.21	273	100	1.04[a]	–	[91]
13X zeolite binderless	4	323	500	1.16[a]	–	[3]
13X zeolite binderless	3.8	323	100	1.23[a]	-37.8[b]	[3]
Zr-fum-MOF	3.6	298	101	1.95[a]	-38[b]	[92]
ZIF-71	3.52	293	101	1.07[a]	-33.4[c]	[86]
13X zeolite from CECA	3.47	323	500	1.13[a]	–	[93]
ZIF-8	3.31	298	100	1.1[a]	–	[90]
13X zeolite from CECA	3.3	323	100	1.2[a]	-53[b]	[93]
NKU-FlexMOF-1a	3.3	273	100	1.2[a]	-56[b]	[94]
IFP-1	3.2	303	101	1.23[a]	-35.4[i]	[71]
Z10-04	3.2	298	100	22.5[f]	–	[95]
13X-APG	2.92[c]	298	100	1.26[a]	-48.5[d]	[6]
$CaNH_4$-Al-LEV	2.8	298	101	5[a]	–	[96]
MPI	2.69	298	101	1.6[f]	-34[b]	[13]
IFP-7	2.55	303	101	1.16[a]	-40[i]	[71]
IFP-5	2.5	303	101	1.22[a]	-34.5[i]	[71]
ZIF-7	2.48	298	101	1.2[a]	–	[83, 97]
13X zeolite	2.45	333	100	1.2[a]	-42.4[e]	[98]
$NaNH_4$-Al-LEV	2.4	298	101	8[a]	–	[96]
ITQ-29	2.34	298	90	1.06[a]	–	[99]
$Zn(ox)_{0.5}(trz)$	2.33	303	101	860[h]	-43[m]	[100]
$CaNH_4$-FeAl-LEV	2.2	298	101	11[a]	–	[96]
Zeolite 5A(UOP)	2.2	298	100	2.9[f]	–	[95]
Si-CHA zeolite	2.1	373	101	44[l]	-29.96[b]	[101]
CMS	2.03	363	100	2.32[a]	–	[102]
Y-abtc	2	298	101	40[a]	-50[b]	[103]
HMS type mesoporous silica	1.94	303	101	1.6[b]	-55.6[c]	[18]

Silica SBA-15	1.94	303	101	1.6[a]	-14.8[b]	19
AlPO4-14	1.9	343	400	15[a]	–	104
$NaNH_4$-FeAl-LEV	1.85	298	101	9.25[a]	–	96
CPL-1	1.82	273	100	6[a]	–	105
4Å (CECA) zeolite	1.8	423	80	60[a]	-45[b]	106
$Zn(ox)_{0.5}$(atrz)	1.71	303	101	175[h]	–	100
HiSiv 3000	1.7[c]	298	100	1[a]	-47.7[d]	6
IFP-3	1.7	303	101	1.2[a]	-34.2[i]	71
ZnMOR-mIM	1.70	298	101	75[f]	–	107
ZnMOR-eIM	1.63	298	101	118[f]	–	107
Z58-3	1.61	298	101	3.4[a]	–	108
Z58-5	1.61	298	101	2.9[a]	–	108
ITQ-50	1.61	298	90	1.38[a]	–	99
Z58	1.61	298	101	7.3[a]	–	108
3SiPPH(0.2)	1.6	293	65	1.45[b]	-45[c]	109
Cu^+-SiPPH723	1.6	293	65	1.8[b]	-19.5[c]	109
Z58-1	1.58	298	101	6.1[a]	–	108
Z58-2	1.56	298	101	4.7[a]	–	108
ZnMOR-pIM	1.52	298	101	139[f]	–	107
SBA-15	1.5	293	40	1.5[a]	-36[b]	110
ELM-12	1.45	298	101	1.5[f] – 204[h]	-30[b]	111
NbOFFIVE-1-Ni	1.43	298	100	18[a]	-57.4[k]	112
$A_{10}B_1$	1.4	298	80	1.7[f] – 1.19[a]	–	16
MAF-23-O	1.4	298	101	9[f] – 15[a]	-54[b]	113
ITQ-12	1.29	303	80	2.45[a]	-40.9[j]	114
AlPO4-14	1.25	343	100	12.5[a]	–	104
DD3R	1.25	318	101	12.5[a]	–	115
ITQ-32 zeolite	1.22	298	100	1.36[a]	–	116
MUV-3	1.12	298	100	1.1[a]	–	90
Cu^{2+}-3SiPPH723	1	293	65	1.3[b]	-27.5[c]	109
MPI-S	0.96	298	101	3.8[f]	-41.2[b]	13
ETS-10	0.83	311	20	1.11[a]	–	117
CPL-1	0.32	298	100	2.08[a]	-22.81[g]	105

[a] Determined from reported adsorption capacities of both gases (propene/propane uptake ratio). [b] Calculated by applying Clausius−Clapeyron equation to adsorption isotherms at different temperatures (value shown is at low surface coverage). [c] Obtained from simulations based on the UFF. [d] Measured/calculated using unconventional method, check the reference for details. [e] Calculated by fitting the experimental adsorption equilibrium data to Toth Model. [f] Calculated using ideally absorbed solution theory (IAST) for an equimolar amount of propene and propane at the responding temperature and pressure. [g] Determined from temperature-programmed desorption (TPD) measurements. [h] Kinetic electivity. [i] Calculated from the Widom Insertion Method. [j] Measurement method not shown/available. [k] Measured using differential scanning calorimetry (DSC). [l] Overall selectivity (equilibrium and kinetic terms). [m] Calculated by using the virial equation.

Table S9. Comparison between the propene uptake, propene/propane selectivity, and heat of adsorption of the propene selective porous with open metal sites adsorbents reported in this review.

Material	Propene Uptake ($mmol_{propene}/g_{material}$)	Temperature (K)	Pressure (kPa)	Propene/Propane Selectivity	Heat of Adsorption ($kJ/mol_{propene}$)	Reference
Cr_3 cluster@MIL-101(Cr)	9.5	273	100	1.8[c]	-28[d]	118
CuBTC(M1)	9.1	303	100	1.12[a] – 3.2[f]	-49[d]	119
Mg-MOF-74	8.3	298	100	1.19[a] – 8.9[c]	-52.6[d]	25
KRICT Cu-BTC spheres	8	323	500	1.14[a]	–	120
MIL-101(Cr)	7.85	303	101	1.5[c]	-36.9[d]	39
Mg_2(dhtp)	7.8	295	101	1.22[a]	–	28
MIL-101(Cr)_DAA	7.6	303	101	2.2[c]	-49.1[d]	39
Co_2(m-dobdc)	7.5	298	101	40[c]	-54[d]	26
MIL-100(Fe)	7.5	298	101	5[c]	-80[d]	33
Mg_2(dobdc)	7.49	318	101	5.55[c]	-47.5[d]	30
KRICT Cu-BTC spheres	7.35	323	100	1.19[a]	-47[d]	120
Fe_2(m-dobdc)	7.3	298	101	56[c]	-74[d]	26
Ni_2(m-dobdc)	7.3	298	101	35[c]	-55[d]	26
Co-MOF-74	7.29	298	101	1.38[a] – 46[c]	-49[e]	27
Mn_2(dobdc)	7.23	318	101	16.6[c]	-48.5[d]	30
Mn_2(m-dobdc)	7.1	298	101	40[c]	-68[d]	26
MgMOF-74	7.1	296	101	10.67[c]	-55[b]	29
Ni_2(dobdc)	6.96	318	101	10.4[c]	-47.5[d]	30
Fe_2(dobdc)	6.9	318	101	14.7[c]	-44[d]	30
Co_2(dobdc)	6.84	318	101	8.63[c]	-45[d]	30
Co_2(dobdc)	6.7	298	101	14.2[c] – 1.13[a]	-82.1[d]	121
Zn_2(dobdc)	6.31	318	101	3.89[c]	-47.5[d]	30
Mn-MOF-74	6	298	101	1.4[a] – 24[c]	-45.1[e]	27
Mg-MOF-74	5.9	298	101	1.37[a] – 4.5[c]	-44.8[d]	27
MC-S-Ag-3	5.5	298	101	2.4[c]	–	36
Co_2(dhtp)	4.9	295	101	1.36[a]	–	28
CoMOF-74	4.9	296	101	8.63[c]	-54[d]	29
(Cr)-MIL-101-SO_3H	4.54	303	101	1.83[c]	-41[d]	40
MIL-100(Fe)	4.5	323	100	1.15[a] – 4.5[c]	–	122
(Cr)-MIL-101-SO_3Ag	4.32	303	101	32[c]	-101[d]	40
NaX	3.99	318	100	1.06[a] – 20[c]	-52[b]	123
CuA_2B_1	3.91	298	80	2.7[c] – 1.3[a]	–	16
NaY	3.7	298	100	12[a]	–	124
LTA5A	3	298	100	30[a]	–	124
Cu-BTC extrudates	2.9	323	100	1.16[a]	-51[d]	125
Ag2SiAl20	2.8	298	101	1.9[a]	–	126
Cu2SiAl20	2.8	298	101	2.3[a]	–	126
GeFSIX-2-Cu-i	2.69	298	101	4[c] – 1.49[a]	-36.25[d]	127
SIFSIX-2-Cu-i	2.65	298	101	5[c] – 1.59[a]	-35.82[d]	127
Cu10SiAl20	2.15	298	101	1.6[a]	–	126
SiAl20Ag5	2.15	298	101	2[a]	–	126
Ag5SiAl20	2.1	298	101	4.1[a]	–	126
Ag10SiAl20	2.1	298	101	1.6[a]	–	126
SiAl20Ag2	2.1	298	101	1.8[a]	–	126

SiAl20Ag20	2	298	101	2[a]	–	126
Cu5SiAl20	2	298	101	1.8[a]	–	126
Co(AIP)(BPY)$_{0.5}$	1.99	298	100	21[c]	-42.5[d]	128
Cu20SiAl20	1.95	298	101	1.7[a]	–	126
SiAl20Cu2	1.95	298	101	1.8[a]	–	126
[Zn_2(5-aip)$_2$(bpy)]·(DMF)·(H_2O)$_2$	1.91	298	100	19.8[c]	-46.2[d]	129
SiAl20Ag10	1.9	298	101	2.2[a]	–	126
Li-FER-27.5	1.85	303	80	2.3[c]	-80.9[d]	130
SiAl20Cu5	1.85	298	101	1.9[a]	–	126
Na-ETS-10 (lab synthesised)	1.75	298	100	7.5[c]	–	95
Na-FER-27.5	1.69	303	80	2.3[c]	-76.8[d]	130
$CuA_{10}B_1$	1.65	298	80	10.4[c] – 1.77[a]	–	16
K-FER-27.5	1.63	303	80	3.8[c]	-66.1[d]	130
$AgNO_3$/MCM-41	1.61	343	101	–	–	23
Ag20SiAl20	1.45	298	101	2[a]	–	126
Na-FER-8.6	1.43	303	80	2.6[c]	-80.4[d]	130
K-FER-8.6	1.42	303	80	71.2[c]	-77.6[d]	130
Li-FER-8.6	1.42	303	80	2.5[c]	-79.8[d]	130
SiAl10Cu	1.4	298	100	1.5[a]– 1.7[c]	–	131
Olesorb-1	1.39	303	101	4.6[a]	-59.83[d]	52
SiAl5Cu	1.35	298	100	1.6[a] – 1.8[c]	–	131
Ag^+ Resin	1.29	298	101	10.4[a]	-43.1[b]	53
SiAl5Ag	1.25	298	100	1.6[a] – 2.2[c]	–	131
AGTU-3a	1.22	298	100	13[c]	-68[d]	132
SiAl20Ag20$_{IM}$	1.21	298	30	5.3[a]	-111.5[b]	133
SiAl10Ag	1.21	298	100	1.8[a] – 2.4[c]	–	131
SiAl20Cu10	1.2	298	101	1.8[a]	–	126
SiAl20Cu$_{red}$	1.15	298	100	2[a] – 2.4[c]	–	131
SiAl20Ag	1.12	298	100	1.9[a]– 4.4[c]	–	131
Cu/SBA-15	1.1	293	40	1.83[a]	-50[d]	110
SiAl20Cu7$_{EX}$	1.1	298	30	2.39[a]	–	133
MPI-Ag	1.07	298	101	7.2[c]	-46.8[d]	13
Ag-ETS-10-25	1.02	311	20	1.34[a]	–	117
SiAl20Cu	1	298	100	1.5[a] – 1.8[c]	–	131
SiAl20Cu10$_{DI}$	1	298	30	1.6[a]	-42.2[b]	133
Ag-ETS-10-8	0.99	311	20	1.14[a]	–	117
SiAl20Ag20$_{EX}$	0.9	298	30	3.2[a]	-73.2[b]	133
SiAl20Cu20	0.9	298	101	1.8[a]	–	126
SiAl20Ag20$_{DI}$	0.8	298	30	1.9[a]	-89.4[b]	133
SiAl20Cu10$_{IM}$	0.6	298	30	1.58[a]	-23.8[b]	133

[a] Determined from reported adsorption capacities of both gases (propene/propane uptake ratio). [b] Measurement method not shown/available. [c] Calculated using ideally absorbed solution theory (IAST) for an equimolar amount of propene and propane at the responding temperature and pressure. [d] Calculated by applying Clausius−Clapeyron equation to adsorption isotherms at different temperatures (value shown is at low surface coverage). [e] Measured/calculated using unconventional method, check the reference for details. [f] Determined from breakthrough data.

Table S10. Comparison between the propene uptake, propene/propane selectivity, and heat of adsorption of the propene selective nonporous adsorbents reported in this review.

Material	Propene Uptake ($mmol_{propene}/g_{material}$)	Temperature (K)	Pressure (kPa)	Propene/Propane Selectivity	Heat of Adsorption ($kJ/mol_{propene}$)	Reference
Cu(0.6)@MIL-100(Fe)	3.4	323	100	1.62[a] – 13[e]	–	122
[Cu-H]$_3$	2.8[c]	293	519	29[d]	–	59
37.5 wt% $AgNO_3$/silica	2.7	298	295	3.86[a]	–	134
$AgNO_3/SiO_2$	2.4	298	100	3[a]	–	135
39.4 wt% $AgNO_3$/aluminosilica	2.3	298	295	3.29[a]	–	134
39.4 wt% $AgNO_3$/aluminosilica	2.2	298	98	1.83[a]	–	134
[Cu-Br]$_3$	2.09	293	100	39.5[a]	-17[b]	59
37.5 wt% $AgNO_3$/aluminosilica	2.05	298	295	2.05[a]	–	134
36 wt% CuCl/NaX	1.87	318	100	1.33[a] – 100[e]	-59[f]	123
37.5 wt% $AgNO_3$/aluminosilica	1.8	298	98	2.57[a]	-54.8[b]	134
28.5 wt% $AgNO_3$/clay	1.75	298	295	1.84[a]	–	134
[Cu-Br]$_3$	1.49[c]	293	476	27[d]	–	59
$AgNO_3/SiO_2$ (impregnation)	1.49	343	101	4.3[a]	–	23
$AgNO_3$/clay adsorbent	1.3	298	101	4.3[a]	–	63
CuCl/γ-Al_2O_3	0.77	298	101	3.5[a]	-59.4[f]	53
1 (fine crystal)	0.23	298	400	150[a]	–	66
[Cu-H]$_3$	<0.1	293	100	<0.1[a]	–	59

[a] Determined from reported adsorption capacities of both gases (propene/propane uptake ratio). [b] Calculated by applying Clausius−Clapeyron equation to adsorption isotherms at different temperatures. [c] Pressure drop method for 120 min. [d] Selectivity calculated from capacities measured by pressure drop method. [e] Calculated using ideally absorbed solution theory (IAST) for an equimolar amount of propene and propane at the responding temperature and pressure. [f] Measurement method not shown/available.

2.5 Propane selective adsorbents

Table S11. Comparison between the propane uptake, propane/propene selectivity, and heat of adsorption of the propane selective porous adsorbents reported in this review.

Material	Propane Uptake ($mmol_{propane}/g_{material}$)	Temperature (K)	Pressure (kPa)	Propane/Propene Selectivity	Heat of Adsorption ($kJ/mol_{propane}$)	Reference
Kureha carbon	3.1	273	2	1.15[a]	-41.5[b]	[2]
MOF-801 (with defects)	1.63	298	101	1.28[a]	-44[b]	[92]
ZIF-4	2.4	293	101	1.25[c]	–	[81]
ZIF-9	2.63	293	101	1.02[a]	-56.46[d]	[86]
ZIF-67	3.1	298	50	1.42[a]	–	[91]
ZIF-71	2.65	293	50	1.1[a]	-36.4[d]	[86]

[a] Determined from reported adsorption capacities of both gases (propane/propene uptake ratio). [b] Calculated by applying Clausius−Clapeyron equation to adsorption isotherms at different temperatures (value shown is at low surface coverage). [c] Calculated using ideally absorbed solution theory (IAST) for an equimolar amount of propane and propene at the responding temperature and pressure. [d] Obtained from simulations based on the UFF.

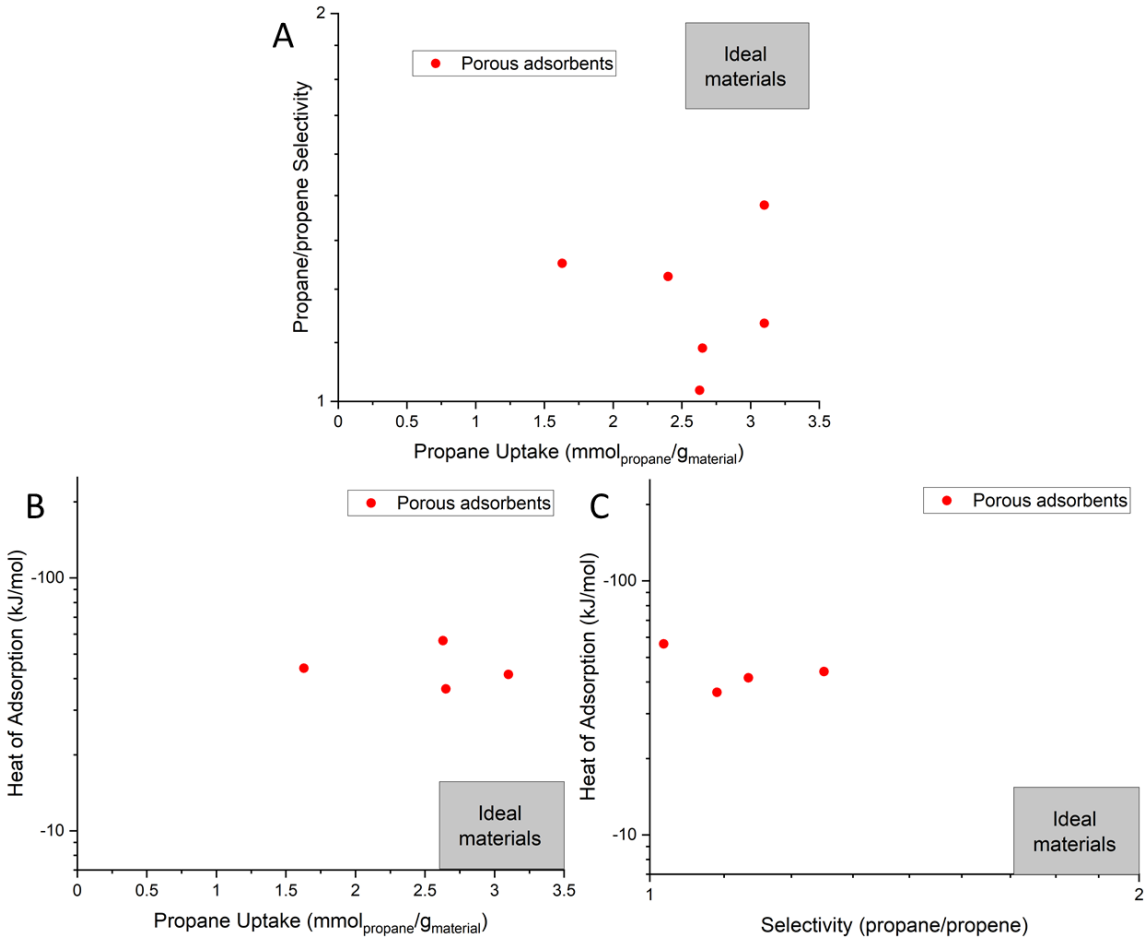

Figure S3. Bound plots for propane selective adsorbents. Note: there are too few data points to draw 'bound' lines. A) Correlation illustrating the trade-off between uptake and selectivity in adsorbents characterized for propane/propene separations. B) Correlation illustrating the trade-off between uptake and heat of adsorption in adsorbents characterized for propane/propene separations. C) Correlation illustrating the trade-off between selectivity and heat of adsorption in adsorbents characterized for propane/propene separations.

2.6 Breakthrough data for adsorbents used for propene/propane separation

Table S12. Breakthrough data for propene selective adsorbents reported in this review.

Material	Temperature (K)	Pressure (kPa)	Breakthrough Time (min)	Alkene Productivity (L/Kg)	Propene Heat of Adsorption (kJ/mol)	Reference
36 wt% CuCl/NaX	318	100	0/ 0.5[s]	–	-47.8[e]	123
4A zeolite	423	500	–[a]	1.03[m,u]	–	136
13X zeolite	423	500	–[a]	0.785[m,v]	-35.8[e]	137
13X zeolite from CECA	373	150	10.8 / 13.7[l]	1.46[i,m]	-53[d]	93
AGTU-3a	298	100	16 / 19.5[a]	5[b]	-68[d]	132
Co_2(dhtp)	295	101	62 / 99[a]	–	–	28
Co_2(m-dobdc)	318	101	90 / 140[a]	–	-54[d]	26
Co(AIP)(BPY)$_{0.5}$	298	100	2.47 / 5.3[a]	–	-42.5[d]	128
CoMOF-74	296	100	–	3.48[i,j]	-54[d]	29
Co-MOF-74	298	101	180 / 325[a]	145.6[b]	–	113
CPL-1	273	100	4 / 7[a]	40.77[b]	–	105
CPL-1	298	100	2.5 / 4[a]	7.17[b]	–	105
Cr_3 cluster@MIL-101(Cr)	303	100	7 / 9[a]	–	-28[d]	118
Cu(0.6)@MIL-100(Fe)	323	100	0.97 / 2[a]	–	–	122
CuBTC(M1)	313	100	20 / 60[r]	–	-49[d]	119
DD3R	323	101	0 / 1.7[a]	–	–	115
ELM-12	298	101	15 / 30[a]	–	-30[d]	111
Fe_2(dobdc)	318	100	33 / 55[a]	4[i,j]	-44[d]	31
FeMOF-74	318	100	–	3.64[i,j]	-55[d]	29
KAUST-7	298	101	13 / 51[a]	26[b]	–	113
KRICT Cu-BTC spheres	373	150	10.8 / 14.2[o]	0.6[m,p]	-47[d]	120
MAF-23-O	298	101	37 / 97[a]	29.12[b]	-54[d]	113
MC-S-Ag-3	298	100	380 / 520[c]	–	–	36
Mg_2(dhtp)	295	101	21 / 28[a]	–	–	28
MgMOF-74	296	100	–	3.27[i,j]	-55[d]	29
MIL-100(Fe)	323	100	0.67 / 1.13[a]	–	–	122
MIL-101(Cr)_DAA	303	101	0.5 / 0.85[a]	–	-49.1[d]	39
NaX	318	100	8.3 / 15[s]	–	-52[e]	123
NbOFFIVE-1-Ni	298	100	0 / 8.5[a]	13.44[b]	-57.4[t]	112
NKU-FlexMOF-1a	298	100	24 / 50[a]	43.9[k]	-56[d]	94
Y-abtc	298	101	1 / 13[a]	–	-50[d]	103
Z58	298	101	0 / 1.58[a]	–	–	108
Z58-1	298	101	0 / 1.58[a]	–	–	108
Z58-2	298	101	0 / 1.83[a]	–	–	108
Z58-3	298	101	0 / 3.16[a]	–	–	108

Z58-5	298	101	0 / 3.16[a]	–	–	[108]
[Zn_2(5-aip)$_2$(bpy)]·(DMF)·(H_2O)$_2$	298	100	4 / 6[a]	–	-46.2[d]	[129]
Zn_2Cu_3(BTDD)$_3$	296	101	0.2 / 3.2[a]	–	–	[34]
ZnMOR-eIM	298	101	3 / 13[a]	10.53[b]	–	[107]
ZnMOR-mIM	298	101	2.5 / 9[a]	6.94[b]	–	[107]
ZnMOR-pIM	298	101	3.2 / 14.5[a]	11.87[b]	–	[107]

[a] Breakthrough cycle of equimolar alkane/alkene (50:50) mixture. [b] Purity not shown/available. [c] Dimensionless time. [d] Calculated by applying Clausius−Clapeyron equation to adsorption isotherms at different temperatures (value shown is at low surface coverage). [e] Measurement method not shown/available. [f] Purity over 99.99%. [g] Purity over 99.95%. [h] Purity over 99.2%. [i] Purity over 99.5%. [j] Productivity is expressed as mol of alkene per L of adsorbent. [k] Purity over 85.2%. [l] Breakthrough cycle of a mixture of 25% propane and 75% propene. [m] Productivity is expressed as mol of alkene per kg of adsorbent per hour. [n] Breakthrough cycle of a mixture of propane/propene/nitrogen (10:10:80). [o] Breakthrough cycle of a mixture of 70% propane and 30% propene. [p] Purity over 99.8%. [q] Breakthrough cycle of a mixture of 41% propane and 59% propene. [r] Breakthrough cycle of a mixture of propane/propene/helium (2.5:2.5:95). [s] Breakthrough cycle of a mixture of alkane/alkene/helium (25:25:50). [t] Measured using differential scanning calorimetry (DSC). [u] Purity of 97%. [v] Purity of 98%.

Table S13. Breakthrough data for propane selective adsorbents reported in this review.

Material	Temperature (K)	Pressure (kPa)	Breakthrough Time (min)	Alkene Productivity (L/Kg)	Propane Heat of Adsorption (kJ/mol)	Reference
MOF-801 (with defects)	298	101	19 / 18[a]	–	-44[b]	[92]

[a] Breakthrough cycle of equimolar alkane/alkene (50:50) mixture. [b] Calculated by applying Clausius−Clapeyron equation to adsorption isotherms at different temperatures (value shown is at low surface coverage).

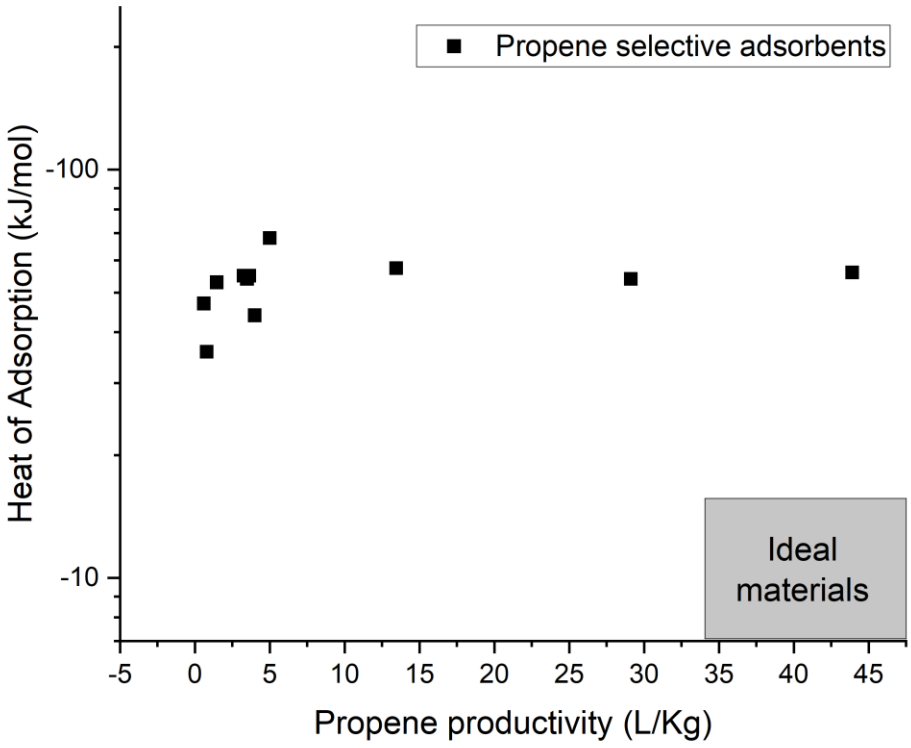

Figure S4. Bound plot for propene selective adsorbents tested for breakthrough measurements. Note that no real conclusions can be drawn from this data due to the variance in measurement conditions and judgement of the purity that defines 'breakthrough.'

2.7 Butene selective adsorbents

Table S14. Comparison between the butene uptake, butene/butane selectivity, and heat of adsorption of the butene selective porous adsorbents reported in this review.

Material	Butene Uptake ($mmol_{butene}/g_{material}$)	Temperature (K)	Pressure (kPa)	Butene/Butane Selectivity	Heat of Adsorption (kJ/mol_{butene})	Reference
Norit R1 Extra	5.87[a]	298	100	1.09[b]	-48.3[a]	6
AC (F30/470)	4.04	293	106.2	1.072[b]	–	138
13X-APG	2.37[a]	298	100	1.16[b]	-56.7[a]	6
HiSiv 3000	1.63[a]	298	100	1.052[b]	-57.5[a]	6
ITQ-32 zeolite	0.75	333	30.4	7.5[b]	–	116

[a] Measured/calculated using unconventional method, check the reference for details. [b] Determined from reported adsorption capacities of both gases (butene/butane uptake ratio).

Table S15. Comparison between the butene uptake, butene/butane selectivity, and heat of adsorption of the butene selective porous with open metal sites adsorbents reported in this review.

Material	Butene Uptake ($mmol_{butene}/g_{material}$)	Temperature (K)	Pressure (kPa)	Butene/Butane Selectivity	Heat of Adsorption (kJ/mol_{butene})	Reference
Cu-BTC	8.1	298	100	1.1[a]	–	139
Fe–Cu/MCM-41	4.4	313	101	2.59[a]	-23.4[c]	140
$[Cu_4(\mu_4O)(\mu_2OH)_2(Me_2trz\text{-}pba)_4]$	4.1	298	99.7	1.085[a]	-45.6[b]	141
Cu-MOF1	3.5	273	101	1.09[a]	-21[b]	88
Cu/MCM-41	2.8	313	101	1.49[a]	-11.2[c]	140
$AgNO_3$/clay	0.92	353	120	2.94[a]	-75.3[b]	142

[a] Determined from reported adsorption capacities of both gases (butene/butane uptake ratio). [b] Calculated by applying Clausius−Clapeyron equation to adsorption isotherms at different temperatures (value shown is at low surface coverage). [c] Calculated by applying the Arrhenius equation to the adsorption isotherms at different temperatures.

Table S16. Comparison between the butene uptake, butene/butane selectivity, and heat of adsorption of the butene selective nonporous adsorbents reported in this review.

Material	Butene Uptake ($mmol_{butene}/g_{material}$)	Temperature (K)	Pressure (kPa)	Butene/Butane Selectivity	Heat of Adsorption (kJ/mol_{butene})	Reference
$[Cu\text{-}Br]_3$	2.45[a]	293	162	–	–	143
$[Cu\text{-}H]_3$	1.05[a]	293	182	–	–	143
$[Cu\text{-}H]_3$	0.53[a]	293	100	–	–	143
$[Cu\text{-}Br]_3$	0.44[a]	293	100	–	–	143

[a] Pressure drop method for 120 min.

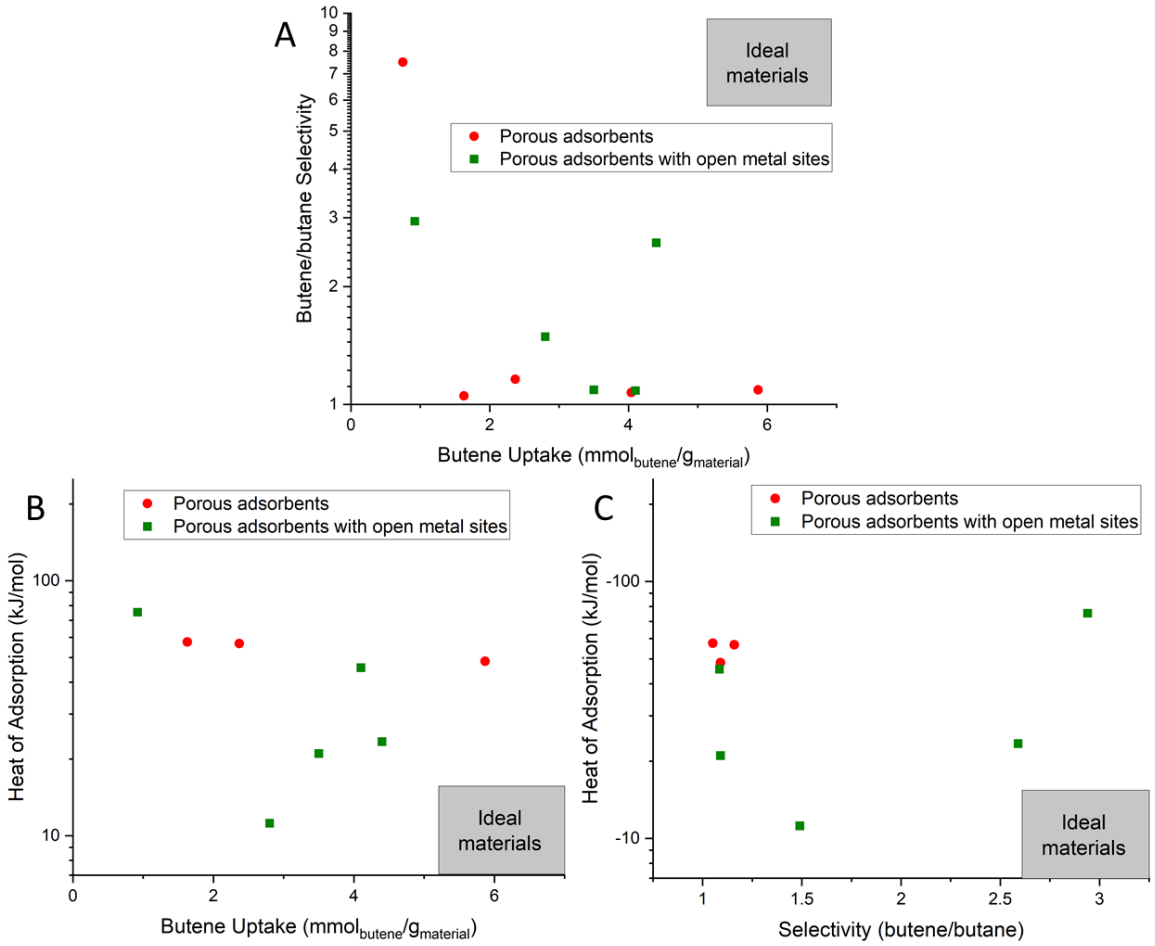

Figure S5. Bound plots for butene selective adsorbents. Note: there are too few data points to draw 'bound' lines. A) Correlation illustrating the trade-off between uptake and selectivity in adsorbents characterized for butene/butane separations. B) Correlation illustrating the trade-off between uptake and heat of adsorption in adsorbents characterized for butene/butane separations. C) Correlation illustrating the trade-off between selectivity and heat of adsorption in adsorbents characterized for butene/butane separations.

3. References

1. L. Huang and D. Cao, *J. Mater. Chem. A,* , 2013, **1**, 9433-9439.
2. W. Zhu, J. Groen, A. Van Miltenburg, F. Kapteijn and J. Moulijn, *Carbon*, 2005, **43**, 1416-1423.
3. G. Narin, V. F. Martins, M. Campo, A. M. Ribeiro, A. Ferreira, J. C. Santos, K. Schumann and A. E. Rodrigues, *Sep. Purif. Technol.*, 2014, **133**, 452-475.
4. Y. He, Z. Zhang, S. Xiang, F. R. Fronczek, R. Krishna and B. Chen, *Chem. Eur. J.*, 2012, **18**, 613-619.
5. S. Pu, J. Wang, L. Li, Z. Zhang, Z. Bao, Q. Yang, Y. Yang, H. Xing and Q. Ren, *Ind. Eng. Chem. Res.*, 2018, **57**, 1645-1654.
6. C. Bläker, C. Pasel, M. Luckas, F. Dreisbach and D. Bathen, *Microporous Mesoporous Mater.*, 2017, **241**, 1-10.
7. K. Kishida, S. Horike, Y. Watanabe, M. Tahara, Y. Inubushi and S. Kitagawa, *Chem. Asian J.*, 2014, **9**, 1643-1647.
8. F. Gao, Y. Wang, X. Wang and S. Wang, *J. Porous Mater.*, 2017, **24**, 713-719.
9. R.-B. Lin, L. Li, H.-L. Zhou, H. Wu, C. He, S. Li, R. Krishna, J. Li, W. Zhou and B. Chen, *Nat. Mater.*, 2018, **17**, 1128-1133.
10. M. Mofarahi and S. M. Salehi, *Adsorption*, 2013, **19**, 101-110.
11. G. Chang, Z. Bao, Q. Ren, S. Deng, Z. Zhang, B. Su, H. Xing and Y. Yang, *RSC Adv.*, 2014, **4**, 20230-20233.
12. Y. Yin, Z. Zhang, C. Xu, H. Wu, L. Shi, S. Wang, X. Xu, A. Yuan, S. Wang and H. Sun, *ACS Sustain. Chem. Eng.*, 2019, **8**, 823-830.
13. J. Yan, B. Zhang, L. Guo and Z. Wang, *J. Phys. Chem. C*, 2018, **123**, 575-583.
14. L. Yu, W. Chu, S. Luo, J. Xing and F. Jing, *J. Chem. Eng. Data*, 2017, **62**, 2562-2569.
15. Y. Wang, S. Yuan, Z. Hu, T. Kundu, J. Zhang, S. B. Peh, Y. Cheng, J. Dong, D. Yuan and H.-C. Zhou, *ACS Sustain. Chem. Eng.*, 2019, **7**, 7118-7126.
16. M. H. Weston, Y. J. Colón, Y.-S. Bae, S. J. Garibay, R. Q. Snurr, O. K. Farha, J. T. Hupp and S. T. Nguyen, *J. Mater. Chem. A*, 2014, **2**, 299-302.
17. A. C. Dewitt, K. Herwig and S. J. Lombardo, *Adsorption*, 2005, **11**, 491-499.
18. B. L. Newalkar, N. V. Choudary, U. T. Turaga, R. P. Vijayalakshmi, P. Kumar, S. Komarneni and T. S. G. Bhat, *Microporous Mesoporous Mater.*, 2003, **65**, 267-276.
19. B. L. Newalkar, N. V. Choudary, P. Kumar, S. Komarneni and T. S. Bhat, *Chem. Mater.*, 2002, **14**, 304-309.
20. C. A. Grande, A. Lind, Ø. Vistad and D. Akporiaye, *Ind. Eng. Chem. Res.*, 2014, **53**, 15522-15530.
21. P. Li, Y. He, H. D. Arman, R. Krishna, H. Wang, L. Weng and B. Chen, *Chem. Comm.*, 2014, **50**, 13081-13084.
22. C. Le and L. Xiaoqin, *Chin. J. Chem. Eng*, 2008, **16**, 570-574.
23. J. Padin and R. T. Yang, *Chem. Eng. Sci.*, 2000, **55**, 2607-2616.
24. V. F. Martins, A. M. Ribeiro, A. Ferreira, U.-H. Lee, Y. K. Hwang, J.-S. Chang, J. M. Loureiro and A. E. Rodrigues, *Sep. Purif. Technol.*, 2015, **149**, 445-456.
25. Z. Bao, S. Alnemrat, L. Yu, I. Vasiliev, Q. Ren, X. Lu and S. Deng, *Langmuir*, 2011, **27**, 13554-13562.
26. J. E. Bachman, M. T. Kapelewski, D. A. Reed, M. I. Gonzalez and J. R. Long, *J. Am. Chem. Soc.*, 2017, **139**, 15363-15370.
27. Y. S. Bae, C. Y. Lee, K. C. Kim, O. K. Farha, P. Nickias, J. T. Hupp, S. T. Nguyen and R. Q. Snurr, *Angew. Chem. Int. Ed.*, 2012, **51**, 1857-1860.
28. U. Böhme, B. Barth, C. Paula, A. Kuhnt, W. Schwieger, A. Mundstock, J. r. Caro and M. Hartmann, *Langmuir*, 2013, **29**, 8592-8600.
29. Y. He, R. Krishna and B. Chen, *Energy Environ. Sci.*, 2012, **5**, 9107-9120.
30. S. J. Geier, J. A. Mason, E. D. Bloch, W. L. Queen, M. R. Hudson, C. M. Brown and J. R. Long, *Chem. Sci.*, 2013, **4**, 2054-2061.

31. E. D. Bloch, W. L. Queen, R. Krishna, J. M. Zadrozny, C. M. Brown and J. R. Long, *Science*, 2012, **335**, 1606-1610.
32. B. Li, Y. Zhang, R. Krishna, K. Yao, Y. Han, Z. Wu, D. Ma, Z. Shi, T. Pham and B. Space, *J. Am. Chem. Soc.*, 2014, **136**, 8654-8660.
33. L. Mei, Y. Wu, X. Zhou, J. Yan, F. Xu and Z. Li, *J. Taiwan Inst. Chem. Eng.* , 2017, **70**, 74-78.
34. M. H. Mohamed, Y. Yang, L. Li, S. Zhang, J. P. Ruffley, A. G. Jarvi, S. Saxena, G. t. Veser, J. K. Johnson and N. L. Rosi, *J. Am. Chem. Soc.*, 2019, **141**, 13003-13007.
35. G. R. Lorzing, B. A. Trump, C. M. Brown and E. D. Bloch, *Chem. Mater.*, 2017, **29**, 8583-8587.
36. D. Saha, B. Toof, R. Krishna, G. Orkoulas, P. Gismondi, R. Thorpe and M. L. Comroe, *Microporous Mesoporous Mater.*, 2020, **299**, 110099.
37. W.-J. Jiang, L.-B. Sun, Y. Yin, X.-L. Song and X.-Q. Liu, *Sep. Sci. Technol.*, 2013, **48**, 968-976.
38. Y. Zhang, B. Li, R. Krishna, Z. Wu, D. Ma, Z. Shi, T. Pham, K. Forrest, B. Space and S. Ma, *Chem. Comm.*, 2015, **51**, 2714-2717.
39. S.-Y. Kim, T.-U. Yoon, J. H. Kang, A.-R. Kim, T.-H. Kim, S.-I. Kim, W. Park, K. C. Kim and Y.-S. Bae, *ACS Appl. Mater. Interfaces*, 2018, **10**, 27521-27530.
40. G. Chang, M. Huang, Y. Su, H. Xing, B. Su, Z. Zhang, Q. Yang, Y. Yang, Q. Ren and Z. Bao, *Chem. Comm.*, 2015, **51**, 2859-2862.
41. C. Gu, N. Hosono, J.-J. Zheng, Y. Sato, S. Kusaka, S. Sakaki and S. Kitagawa, *Science*, 2019, **363**, 387-391.
42. S. Aguado, G. r. Bergeret, C. Daniel and D. Farrusseng, *J. Am. Chem. Soc.*, 2012, **134**, 14635-14637.
43. S. Meng, H. Ma, L. Jiang, H. Ren and G. Zhu, *J. Mater. Chem. A*, 2014, **2**, 14536-14541.
44. M. Shi, A. M. Avila, F. Yang, T. M. Kuznicki and S. M. Kuznicki, *Chem. Eng. Sci.*, 2011, **66**, 2817-2822.
45. A. Anson, Y. Wang, C. Lin, T. Kuznicki and S. Kuznicki, *Chem. Eng. Sci.*, 2008, **63**, 4171-4175.
46. M. Shi, C. C. Lin, T. M. Kuznicki, Z. Hashisho and S. M. Kuznicki, *Chem. Eng. Sci.*, 2010, **65**, 3494-3498.
47. Y. Wang, Z. Hu, Y. Cheng and D. Zhao, *Ind. Eng. Chem. Res.*, 2017, **56**, 4508-4516.
48. K. Kishida, Y. Watanabe, S. Horike, Y. Watanabe, Y. Okumura, Y. Hijikata, S. Sakaki and S. Kitagawa, *Eur. J. Inorg. Chem.*, 2014, **2014**, 2747-2752.
49. L. Zhang, L. Li, E. Hu, L. Yang, K. Shao, L. Yao, K. Jiang, Y. Cui, Y. Yang and B. Li, *Adv. Sci.*, 2020, **7**, 1901918.
50. A. Anson, C. C. H. Lin, T. M. Kuznicki and S. M. Kuznicki, *Chem. Eng. Sci.*, 2010, **65**, 807-811.
51. J.-D. XING, F.-L. JING, W. CHU, H.-L. SUN, L. YU, H. ZHANG and S.-Z. LUO, *Acta Phys. -Chim. Sin.*, 2015, **31**, 2158-2164.
52. N. V. Choudary, P. Kumar, T. S. Bhat, S. H. Cho, S. S. Han and J. N. Kim, *Ind. Eng. Chem. Res.*, 2002, **41**, 2728-2734.
53. R. Yang and E. Kikkinides, *AIChE J*, 1995, **41**, 509-517.
54. C. Wu, J. Wang, Y. Fang, Z. Wang, D. Fei, X. Han and Y. Dang, *J. Chem. Eng. Data*, 2019, **64**, 611-618.
55. Z. Wu and Y. Liu, *Chin. J. Chem. Eng*, 2002, **10**, 304-310.
56. H. Xiang, A. Ameen, J. Shang, Y. Jiao, P. Gorgojo, F. R. Siperstein and X. Fan, *Microporous Mesoporous Mater.*, 2020, **293**, 109784.
57. C. Yu, M. G. Cowan, R. D. Noble and W. Zhang, *Chem. Comm.*, 2014, **50**, 5745-5747.
58. F. Gao, Y. Wang, X. Wang and S. Wang, *Adsorption*, 2016, **22**, 1013-1022.
59. D. Parasar, A. H. Elashkar, A. A. Yakovenko, N. B. Jayaratna, B. L. Edwards, S. G. Telfer, H. R. Dias and M. G. Cowan, *Angew. Chem. Int. Ed.*, 2020, **59**, 21001-21006.
60. N. B. Jayaratna, M. G. Cowan, D. Parasar, H. H. Funke, J. Reibenspies, P. K. Mykhailiuk, O. Artamonov, R. D. Noble and H. R. Dias, *Angew. Chem. Int. Ed.*, 2018, **130**, 16680-16684.
61. A. Van Miltenburg, W. Zhu, F. Kapteijn and J. Moulijn, *Chem. Eng. Res. Des.*, 2006, **84**, 350-354.
62. M. G. Cowan, W. M. McDanel, H. H. Funke, Y. Kohno, D. L. Gin and R. D. Noble, *Angew. Chem. Int. Ed.*, 2015, **127**, 5832-5835.
63. S. Cho, S. Han, J. Kim, J. Park and H. Rhee, *Korean J. Chem. Eng.*, 2002, **19**, 821-826.
64. J.-H. Park, S.-S. Han, J.-N. Kim and S.-H. Cho, *Korean J. Chem. Eng.*, 2004, **21**, 236-245.
65. X. Zhou, M. Feng, H. Niu, Y. Song, C. Li and D. Zhong, *Adsorp. Sci. Technol.*, 2016, **34**, 355-367.

66. S. Uchida, R. Kawamoto, H. Tagami, Y. Nakagawa and N. Mizuno, *J. Am. Chem. Soc.*, 2008, **130**, 12370-12376.
67. H. Thakkar, Q. Al-Naddaf, N. Legion, M. Hovis, A. Krishnamurthy, A. A. Rownaghi and F. Rezaei, *ACS Sustain. Chem. Eng.*, 2018, **6**, 15228-15237.
68. M. C. Kroon and L. F. Vega, *Langmuir*, 2009, **25**, 2148-2152.
69. W. Liang, Y. Zhang, X. Wang, Y. Wu, X. Zhou, J. Xiao, Y. Li, H. Wang and Z. Li, *Chem. Eng. Sci.*, 2017, **162**, 192-202.
70. X. Wang, Y. Wu, X. Zhou, J. Xiao, Q. Xia, H. Wang and Z. Li, *Chem. Eng. Sci.*, 2016, **155**, 338-347.
71. M. Hovestadt, S. Bendt, S. S. Mondal, K. Behrens, F. Reif, M. Döpken, H.-J. r. Holdt, F. J. Keil and M. Hartmann, *Langmuir*, 2017, **33**, 11170-11179.
72. J. o. Pires, M. s. L. Pinto and V. K. Saini, *ACS Appl. Mater. Interfaces*, 2014, **6**, 12093-12099.
73. H. Zeng, X.-J. Xie, M. Xie, Y.-L. Huang, D. Luo, T. Wang, Y. Zhao, W. Lu and D. Li, *J. Am. Chem. Soc.*, 2019, **141**, 20390-20396.
74. P.-Q. Liao, W.-X. Zhang, J.-P. Zhang and X.-M. Chen, *Nat. Commun.*, 2015, **6**, 8697.
75. J. Peng, Y. Sun, Y. Wu, Z. Lv and Z. Li, *Ind. Eng. Chem. Res.*, 2019, **58**, 8290-8295.
76. J. Pires, M. L. Pinto, C. M. Granadeiro, A. D. Barbosa, L. Cunha-Silva, S. S. Balula and V. K. Saini, *Adsorption*, 2014, **20**, 533-543.
77. O. T. Qazvini, R. Babarao, Z.-L. Shi, Y.-B. Zhang and S. G. Telfer, *J. Am. Chem. Soc.*, 2019, **141**, 5014-5020.
78. W. Liang, F. Xu, X. Zhou, J. Xiao, Q. Xia, Y. Li and Z. Li, *Chem. Eng. Sci.*, 2016, **148**, 275-281.
79. D. Lv, R. Shi, Y. Chen, Y. Wu, H. Wu, H. Xi, Q. Xia and Z. Li, *ACS Appl. Mater. Interfaces*, 2018, **10**, 8366-8373.
80. H. G. Hao, Y. F. Zhao, D. M. Chen, J. M. Yu, K. Tan, S. Ma, Y. Chabal, Z. M. Zhang, J. M. Dou and Z. H. Xiao, *Angew. Chem. Int. Ed.*, 2018, **130**, 16299-16303.
81. M. Hartmann, U. Böhme, M. Hovestadt and C. Paula, *Langmuir*, 2015, **31**, 12382-12389.
82. M. Hovestadt, S. Friebe, L. Helmich, M. Lange, J. Möllmer, R. Gläser, A. Mundstock and M. Hartmann, *Molecules*, 2018, **23**, 889.
83. C. Gücüyener, J. Van Den Bergh, J. Gascon and F. Kapteijn, *J. Am. Chem. Soc.*, 2010, **132**, 17704-17706.
84. D.-L. Chen, N. Wang, C. Xu, G. Tu, W. Zhu and R. Krishna, *Microporous Mesoporous Mater.*, 2015, **208**, 55-65.
85. P. Krokidas, M. Castier and I. G. Economou, *J. Phys. Chem. C*, 2017, **121**, 17999-18011.
86. S. Bendt, M. Hovestadt, U. Böhme, C. Paula, M. Döpken, M. Hartmann and F. J. Keil, *Eur. J. Inorg. Chem.*, 2016, **2016**, 4440-4449.
87. T. M. Nicholson and S. K. Bhatia, *Adsorp. Sci. Technol.*, 2007, **25**, 607-619.
88. T. Hähnel, G. Kalies, R. Krishna, J. Möllmer, J. Hofmann, M. Kobalz and H. Krautscheid, *Microporous Mesoporous Mater.*, 2016, **224**, 392-399.
89. L. Li, R.-B. Lin, R. Krishna, H. Li, S. Xiang, H. Wu, J. Li, W. Zhou and B. Chen, *Science*, 2018, **362**, 443-446.
90. E. Andres-Garcia, J. López-Cabrelles, L. Oar-Arteta, B. Roldan-Martinez, M. Cano-Padilla, J. Gascon, G. M. Espallargas and F. Kapteijn, *Chem. Eng. J.*, 2019, **371**, 848-856.
91. E. Andres-Garcia, L. Oar-Arteta, J. Gascon and F. Kapteijn, *Chem. Eng. J.*, 2019, **360**, 10-14.
92. P. Iacomi, F. Formalik, J. Marreiros, J. Shang, J. Rogacka, A. Mohmeyer, P. Behrens, R. Ameloot, B. Kuchta and P. L. Llewellyn, *Chem. Mater.*, 2019, **31**, 8413-8423.
93. M. Campo, A. Ribeiro, A. Ferreira, J. Santos, C. Lutz, J. Loureiro and A. Rodrigues, *Sep. Purif. Technol.*, 2013, **103**, 60-70.
94. M.-H. Yu, B. Space, D. Franz, W. Zhou, C. He, L. Li, R. Krishna, Z. Chang, W. Li and T.-L. Hu, *J. Am. Chem. Soc.*, 2019, **141**, 17703-17712.
95. S. Divekar, A. Nanoti, S. Dasgupta, R. Chauhan, P. Gupta, M. O. Garg, S. P. Singh and I. M. Mishra, *J. Chem. Eng. Data*, 2016, **61**, 2629-2637.
96. J. G. Min, K. C. Kemp and S. B. Hong, *Microporous Mesoporous Mater.*, 2020, **294**, 109833.
97. J. van den Bergh, C. Gücüyener, E. A. Pidko, E. J. Hensen, J. Gascon and F. Kapteijn, *Chem. Eur. J.*, 2011, **17**, 8832-8840.
98. N. Lamia, L. Wolff, P. Leflaive, P. Sá Gomes, C. A. Grande and A. E. Rodrigues, *Sep. Sci. Technol.*, 2007, **42**, 2539-2566.

99. J. L. Jordá, F. Rey, G. Sastre, S. Valencia, M. Palomino, A. Corma, A. Segura, D. Errandonea, R. Lacomba and F. J. Manjón, *Angew. Chem. Int. Ed.*, 2013, **52**, 10458-10462.
100. J. Peng, H. Wang, D. H. Olson, Z. Li and J. Li, *Chem. Comm.*, 2017, **53**, 9332-9335.
101. H. Maghsoudi, H. Abdi and A. Aidani, *Ind. Eng. Chem. Res.*, 2020, **59**, 1682-1692.
102. J. Liu, Y. Liu, D. K. Talay, E. Calverley, M. Brayden and M. Martinez, *Carbon*, 2015, **85**, 201-211.
103. H. Wang, X. Dong, V. Colombo, Q. Wang, Y. Liu, W. Liu, X. L. Wang, X. Y. Huang, D. M. Proserpio and A. Sironi, *Adv. Mater.*, 2018, **30**, 1805088.
104. J. Padin, S. U. Rege, R. T. Yang and L. S. Cheng, *Chem. Eng. Sci.*, 2000, **55**, 4525-4535.
105. Y. Chen, Z. Qiao, D. Lv, C. Duan, X. Sun, H. Wu, R. Shi, Q. Xia and Z. Li, *Chem. Eng. J.*, 2017, **328**, 360-367.
106. M. Patiño-Iglesias, G. Aguilar-Armenta, A. Jiménez-López and E. Rodrıguez-Castellón, *Colloids Surf, A Physicochem Eng Asp*, 2004, **237**, 73-77.
107. Y. Wu, S. Zeng, D. Yuan, J. Xing, H. Liu, S. Xu, Y. Wei, Y. Xu and Z. Liu, *Angew. Chem. Int. Ed.*, 2020, **132**, 6831-6834.
108. C. Selzer, A. Werner and S. Kaskel, *Ind. Eng. Chem. Res.*, 2018, **57**, 6609-6617.
109. G. Aguilar-Armenta, M. E. Patiño-Iglesias, J. Jiménez-Jiménez, E. Rodríguez-Castellón and A. Jiménez-López, *Langmuir*, 2006, **22**, 1260-1267.
110. E. Basaldella, J. Tara, G. A. Armenta and M. P. Iglesias, *J. Porous Mater.*, 2007, **14**, 273-278.
111. L. Li, R.-B. Lin, X. Wang, W. Zhou, L. Jia, J. Li and B. Chen, *Chem. Eng. J.*, 2018, **354**, 977-982.
112. A. Cadiau, K. Adil, P. Bhatt, Y. Belmabkhout and M. Eddaoudi, *Science*, 2016, **353**, 137-140.
113. Y. Wang, N. Y. Huang, X. W. Zhang, H. He, R. K. Huang, Z. M. Ye, Y. Li, D. D. Zhou, P. Q. Liao and X. M. Chen, *Angew. Chem. Int. Ed.*, 2019, **131**, 7774-7778.
114. D. H. Olson, X. Yang and M. A. Camblor, *J. Phys. Chem. B*, 2004, **108**, 11044-11048.
115. J. Gascon, W. Blom, A. van Miltenburg, A. Ferreira, R. Berger and F. Kapteijn, *Microporous Mesoporous Mater.*, 2008, **115**, 585-593.
116. M. Palomino, A. Cantín, A. Corma, S. Leiva, F. Rey and S. Valencia, *Chem. Comm.*, 2007, 1233-1235.
117. I. Tiscornia, S. Irusta, P. Prádanos, C. Téllez, J. Coronas and J. Santamaría, *J. Phys. Chem. C*, 2007, **111**, 4702-4709.
118. S. E. Sivan, M. Lee, S. K. Lee, J. W. Yoon, K. Kim, D. Y. Hong, K. H. Cho, U. H. Lee, J. S. Chang and J. Jung, *Chem. Eur. J.*, 2019, **25**, 12889-12894.
119. J.-W. Yoon, I.-T. Jang, K.-Y. Lee, Y.-K. Hwang and J.-S. Chang, *Bull. Korean Chem. Soc.*, 2010, **31**, 220-223.
120. M. Plaza, A. Ribeiro, A. Ferreira, J. Santos, U.-H. Lee, J.-S. Chang, J. M. Loureiro and A. E. Rodrigues, *Sep. Purif. Technol.*, 2012, **90**, 109-119.
121. P. Vervoorts, A. Schneemann, I. Hante, J. Pirillo, Y. Hijikata, T. Toyao, K. Kon, K.-i. Shimizu, T. Nakamura and S.-i. Noro, *ACS Appl. Mater. Interfaces*, 2020, **12**, 9448-9456.
122. A.-R. Kim, T.-U. Yoon, E.-J. Kim, J. W. Yoon, S.-Y. Kim, J. W. Yoon, Y. K. Hwang, J.-S. Chang and Y.-S. Bae, *Chem. Eng. J.*, 2018, **331**, 777-784.
123. A. van Miltenburg, J. Gascon, W. Zhu, F. Kapteijn and J. A. Moulijn, *Adsorption*, 2008, **14**, 309-321.
124. A. Luna-Triguero, A. Sławek, R. Sánchez-de-Armas, J. J. Gutiérrez-Sevillano, C. O. Ania, J. B. Parra, J. M. Vicent-Luna and S. Calero, *Chem. Eng. J.*, 2020, **380**, 122482.
125. A. F. Ferreira, J. C. Santos, M. G. Plaza, N. Lamia, J. M. Loureiro and A. E. Rodrigues, *Chem. Eng. J.*, 2011, **167**, 1-12.
126. M. Kargol, J. Zajac, D. Jones, J. Rozière, T. Steriotis, A. Jiménez-López and E. Rodríguez-Castellón, *Chem. Mater.*, 2005, **17**, 6117-6127.
127. X. Wang, P. Zhang, Z. Zhang, L. Yang, Q. Ding, X. Cui, J. Wang and H. Xing, *Ind. Eng. Chem. Res.*, 2020, **59**, 3531-3537.
128. H. Wu, Y. Yuan, Y. Chen, F. Xu, D. Lv, Y. Wu, Z. Li and Q. Xia, *AIChE J*, 2020, **66**, e16858.
129. Y. Chen, H. Wu, D. Lv, N. Yuan, Q. Xia and Z. Li, *Sep. Purif. Technol.*, 2018, **204**, 75-80.
130. E. Koudelková, Y. Ghrib, F. S. de Oliveira Ramos, P. Čičmanec and R. Bulánek, *Microporous Mesoporous Mater.*, 2019, **279**, 416-422.
131. M. Kargol, J. Zajac, D. Jones, T. Steriotis, J. Roziere and P. Vitse, *Chem. Mater.*, 2004, **16**, 3911-3918.

132. Z. Chang, R.-B. Lin, Y. Ye, C. Duan and B. Chen, *J. Mater. Chem. A*, 2019, **7**, 25567-25572.
133. M. Kargol, J. Zajac, D. Jones and J. Rozière, *Thermochim. Acta*, 2005, **434**, 15-21.
134. C. H. Ko, S.-S. Han, J.-H. Park, S.-H. Cho and J.-N. Kim, *Ind. Eng. Chem. Res.*, 2006, **45**, 9129-9135.
135. S. U. Rege and R. T. Yang, *Chem. Eng. Sci.*, 2002, **57**, 1139-1149.
136. F. A. Da Silva and A. E. Rodrigues, *Ind. Eng. Chem. Res.*, 2001, **40**, 5758-5774.
137. F. A. Da Silva and A. E. Rodrigues, *AIChE J*, 2001, **47**, 341-357.
138. M.-G. Olivier, K. Berlier and R. Jadot, *J. Chem. Eng. Data*, 1994, **39**, 770-773.
139. A. Luna-Triguero, J. Vicent-Luna, A. Poursaeidesfahani, T. Vlugt, R. Sánchez-de-Armas, P. Gómez-Álvarez and S. Calero, *ACS Appl. Mater. Interfaces*, 2018, **10**, 16911-16917.
140. M. Jin, S. S. Kim, Y. D. Kim, J.-N. Park, J. H. Kim, C. H. Ko, J.-N. Kim and J. M. Kim, *J. Mater. Chem. A*, 2013, **1**, 6653-6657.
141. M. Lange, M. Kobalz, J. Bergmann, D. Lässig, J. Lincke, J. Möllmer, A. Möller, J. Hofmann, H. Krautscheid, R. Staudt and R. Gläser, *J. Mater. Chem. A*, 2014, **2**, 8075-8085.
142. J. W. Lee, J. H. Park, S. S. Han, J. N. Kim, S. H. Cho and Y. T. Lee, *Sep. Sci. Technol.*, 2005, **39**, 1365-1384.
143. A. H. Elashkar, D. Parasar, A. Muñoz-Castro, C. M. Doherty, M. G. Cowan and H. R. Dias, *ChemPlusChem*, 2021, **86**, 364-372.